

Simulation of Delamination in a Composite Using a Shell-beam Mesoscale Finite Element Model

DOI: 10.5604/01.3001.0012.1319

University of Bielsko-Biala,
Faculty of Mechanical Engineering
and Computer Science,
ul. Willowa 2, 43-309 Bielsko-Biala, Poland
¹E-mail: jmarszalek@ath.bielsko.pl
²E-mail: jstadnicki@ath.bielsko.pl

Abstract

The article presents a new method of delamination modelling in a fabric-reinforced laminate using a shell-beam mesoscale FE model. This original laminate model enables the analysis of the resistance of composite structures in which the reinforcement can be technical fabric of various weaves or a layer of parallel rovings, e.g. made of carbon fibers. It includes an experimental part in which flat specimens of laminate were delaminated according to three basic schemes: tensile opening, sliding shear and tearing shear. The aim of the experimental studies was to obtain load-displacement curves, which were used to define the conditions of initiation and propagation conditions of cracks in the calculation model as well as to perform their experimental verification. Specimens of the laminate tested were modelled using a mesoscale FE model, in which the components, i.e. the rovings, were modelled in a simplified manner with finite elements of the beam type and a matrix with finite elements of the shell type. The bondings between adjacent laminate layers were also modelled with beam elements. The simulation results were compared with those of experimental delamination tests, and the convergence obtained confirmed the correctness of the modelling method developed.

Key words: woven composite laminate, delamination, experiment, finite element method (FEM), modes of fracture.

Introduction

Laminates reinforced with technical fabrics made of rovings of various fibres are an increasingly common construction material due to their higher strength and resistance to weather conditions. Their multi-phase structure results in the fact that correct determination of the stiffness and strength is more difficult than for metals. Significantly different characteristics of the mechanical properties of the reinforcement (fabric) and matrix (resin) as well as the internal structure of the laminate, which depends on the interlacing of the reinforcement in the fabric and the number and mutual orientation of the reinforcement layers, necessitate the development of discrete computational models of laminates reflecting their mechanical properties in accordance with reality. The discontinuous change in mechanical properties at the interface between the matrix and reinforcement phases is the reason for the most frequently occurring form of damage to laminates subjected to loading – delamination, which in the macroscopic scale is manifested by the break of connection between the layers of the reinforcement. Delamination is a specific structural defect because it is formed inside the laminate. It starts with a small crack caused by excessive stress or finds its origin in inclusions or voids resulting from errors made during lamination (technological defects). The crack may further propagate under loading in

accordance with I, II or III mode of fracture, lowering the strength of the laminate, which consequently leads to destruction (**Figure 1**). During the opening tensile mode caused by the external load N , the crack surfaces move directly apart from each other and the delamination propagates in the direction perpendicular to the front of the crack (**Figure 1.a**). In the sliding shear, the separated surfaces move on each other in a direction perpendicular to the front of the crack as a result of the load T_{yz} (**Figure 1.b**). During scissoring shear, the separated surfaces move on each other in the direction parallel to the front of the crack under the external load T_{xz} (**Figure 1.c**).

In the case where delamination is detected in the laminate structure, it is necessary to decide whether there is a threat to the safety of further operation, so whether a given part should be replaced, fixed, left or not. In the assessment of the risk

of delamination at the design stage, numerical analyses using the finite element method (FEM) are a helpful tool. Modelling of laminates with the use of FEM can be considered on three levels of observation, depending on the degree of details of the computational model.

In the macroscale approach, the laminate is treated as a set of layers whose properties and way of laying determine its stiffness and strength. In practice, they are single-phase solid models which do not take into account the internal structure of the laminate at the component level. The laminate is modelled using finite elements of a solid type [2, 3] and an assumption is made about the homogeneity of the laminate. The laminate is treated as a homogeneous and yet anisotropic material. Material characteristics are obtained in standard experimental tests, such as uniaxial or biaxial tension, compression and shear.

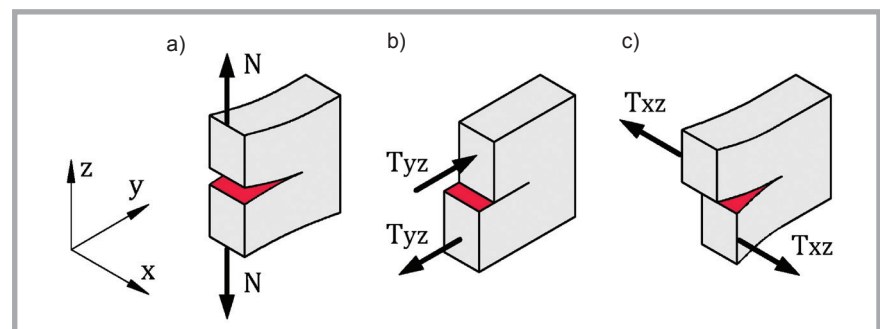


Figure 1. Interlaminar modes of fracture: a) mode I – opening; b) mode II – sliding shear; c) mode III – scissoring shear.

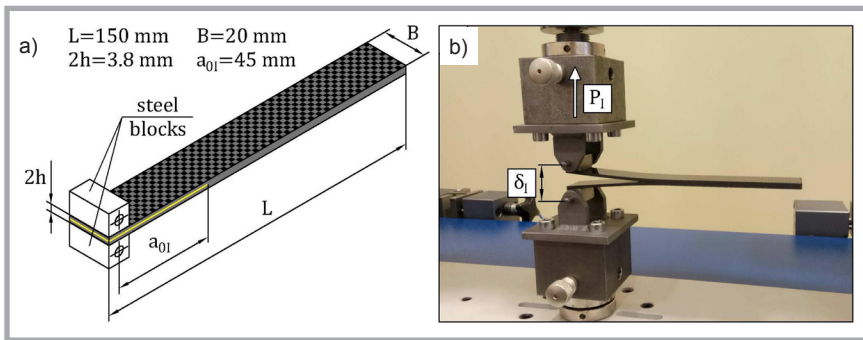


Figure 2. Experimental setup for DCB testing: a) specimen dimensions; b) specimen in the test fixture.

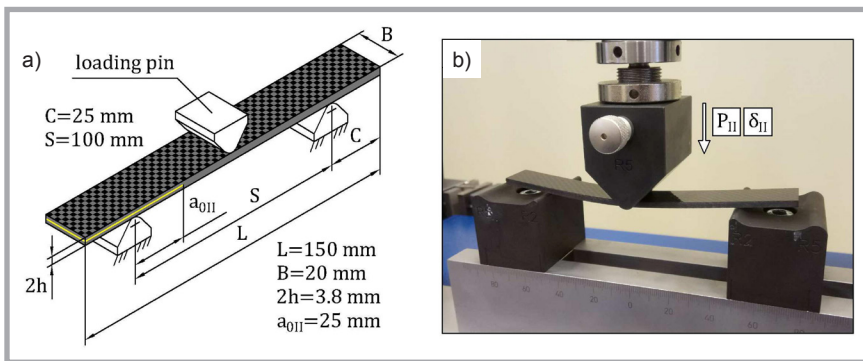


Figure 3. Experimental setup for ENF testing: a) specimen dimensions; b) specimen in the test fixture.

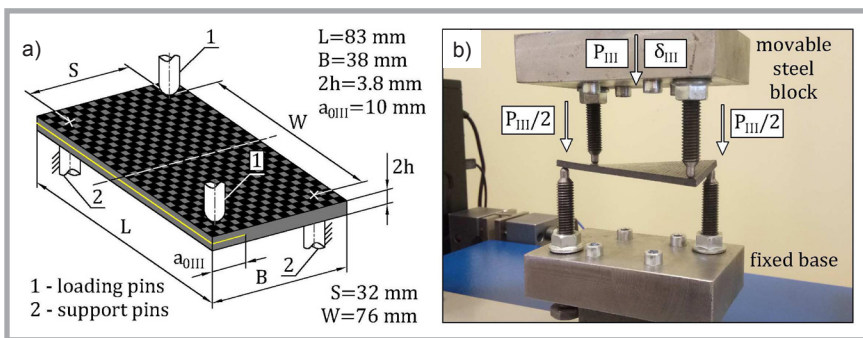


Figure 4. Experimental setup for MECT testing: (a) specimen dimensions; (b) specimen in the test fixture.

Mesoscale discrete models take into account the internal structure of the laminate, with the assumption of homogeneity of the components. The laminate components can be modelled precisely or in a simplified way using finite elements of a solid type [2, 3], shell type [4], beam type [5] and their combination [6].

The last group is made up of microscale models, in which the smallest elements of the laminate structure can be distinguished. These types of models take into account single fibres, between which there is a matrix bonding the model into one whole [7, 8]. Computational models are created from finite elements of a solid type, used to determine the stress distribution at the fibre-matrix phase interface,

to model the propagation of micro-cracks and to analyse the strength of adhesion between the matrix and reinforcing phase. It is worth noting that the numerical efficiency of a computational model of the composite depends on its complexity. In the engineering calculations of structures made of laminates, due to the low numerical efficiency, microscale models are not applicable.

Delamination modelling using the finite element method requires the use of special tools which make it possible to simulate interlayer and interphase connections, which can be removed. One of the ways is the VCCT method (Virtual Crack Closure Technique), which is based on the principles of linear fracture

mechanics and uses in crack propagation modelling the criterion of the threshold value of the energy release rate G [9, 10]. The method, due to the way of calculating parameter G , requires prior definition of the location and shape of the crack front.

Another way of delamination modelling is using the contact debonding method, which comes down to creating a connection between adjacent layers using finite elements of the contact type which can be broken [11, 12]. The criterion of the break takes into account the normal and tangential component of stress in the contact element in relation to threshold normal and tangential values of the breaking stress. After exceeding the criterion, the connection is broken, which is tantamount to the occurrence of a crack. Supplemented with the cracking model, the contact debonding method combines crack initiation criteria based on stress components with the energy criteria of fracture mechanics.

A similar assumption is used in the cohesive zone method, which most often involves the use of an 8-node finite element of the cohesive type, binding adjacent layers of the laminate modelled [13, 14]. Application of the contact debonding method with the cracking model and the cohesive zone method requires defining the relationship between stresses and nodes displacements for the elements modelling the cracking zone.

Experimental investigations

As shown in the first paragraph, a crack in a layered material can propagate according to three modes – opening, sliding shear and scissoring shear (**Figure 1**). A study of laminate resistance to delamination was carried out on flat specimens, with a deliberately initiated pre-crack between the middle layers of the reinforcement. The specimens were cut out from composite plates which were made with the use of the Wet Lay Up method using the same mould tool. Each plate was made of sixteen layers of plain weave fabric of carbon rovings and of epoxy. During the lamination between the middle layers, i.e. between the 8th and 9th layer, a strip of film was inserted which initiated the pre-crack. All experimental tests were carried out on a universal strength testing machine with a maximum force of 5 kN. The dimensions of the laminate specimens (**Figures 2.a, 3.a, 4.a**) and delami-

nating test procedures were selected with the use of literature guidelines [15] and on the basis of standards applicable for unidirectional laminates (ASTM D5528, ASTM D790).

Double cantilever beam test

The assessment of laminate resistance to delamination according to the first fracture mode can be carried out by with the DCB method (double cantilever beam test) with the use of ASTM D5528 standard. The dimensions of the test specimens were $150 \times 20 \times 3.8$ mm and the delamination initiated between the middle layers was 50 mm long (Figure 2.a). The distance a_{0I} of the place corresponding to the application of the external load from the initial delamination front was 45 mm. The fabric layers were arranged in such a way that the reinforcement rovings were parallel and perpendicular to the edge of the specimens (± 90 orientation). Steel blocks were stuck to the specimens, measuring $10 \times 10 \times 20$ mm with a through hole of $\varnothing 5$ mm, into which pins connecting the specimens with the holders of the testing machine were inserted (Figure 2.b). The machine crosshead speed during testing was set at 0.5 mm/min. The parameter applied during the tests was the crack opening δ_I , and the parameter measured was the value of the force P_I .

End-notched flexure test

Testing of the laminate resistance to delamination caused by sliding shear may be carried out in an ENF test (end-notched flexure test), consisting in three-point bending of flat laminate specimens with an initiated pre-crack using ASTM D790 standard. Again test specimens were made with dimensions of $150 \times 20 \times 3.8$ mm (Figure 3.a). In this test, distance a_{0II} is that between the specimen support and pre-crack front. The specimens were loaded in the middle of their length and the supports placed symmetrically in relation to the place of load application (Figure 3.b). During the tests, the deflection of specimens δ_{II} was applied at a speed of 0.5 mm/min, and the parameter measured was the value of force P_{II} .

Edge crack torsion test

Testing of laminate scissoring shear can be carried out in an ECT test (edge crack torsion test), in which the crack front is subjected to torsion. The test procedure has not been standardised as yet, hence the test was carried out according to the

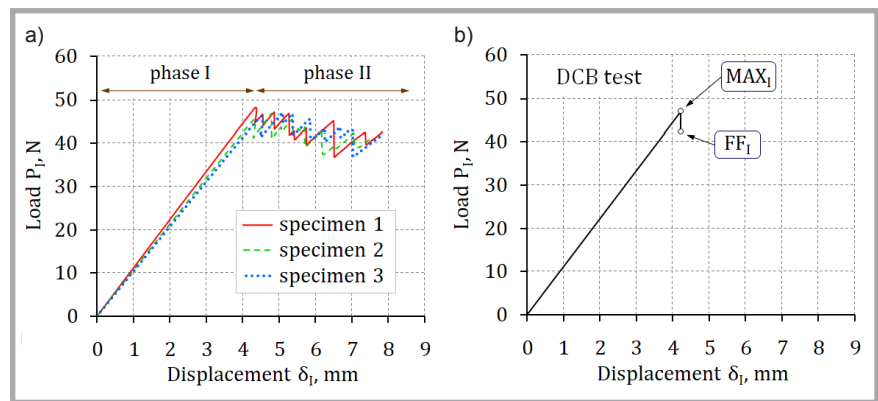


Figure 5. Experimental results for the DCB test: a) in the form of exemplary load-displacement curves, b) in the form of average curve.

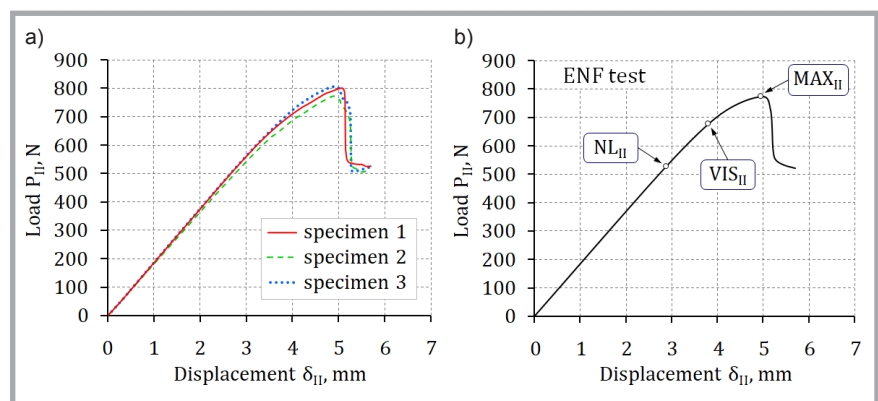


Figure 6. Experimental results for the ENF test: a) in the form of exemplary load-displacement curves, b) in the form of average curve.

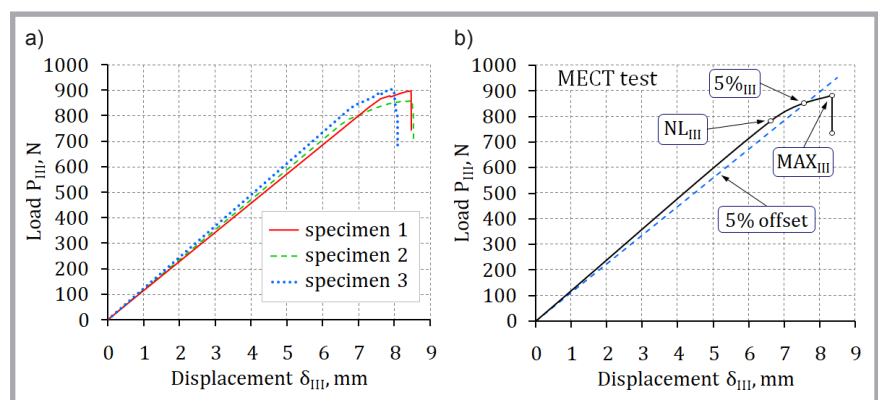


Figure 7. Experimental results for the MECT test: a) in the form of exemplary load-displacement curves, b) in the form of average curve.

recommendations presented in literature [15], which suggests that reinforcement in the specimen should be placed at an orientation of $[90/(\pm 45)_n/(\mp 45)_n/90]_s$. However, for the purposes of this work it was assumed that the reinforcement in the specimens would be arranged in the same way as in those used in previous tests, thus at an orientation of $[\pm 90]$. In the tests, flat specimens with dimensions of $83 \times 38 \times 3.8$ mm were used (Figure 4.a). In each specimen, a pre-crack a_{0III} of 10 mm length was initiated. The tests were

carried out on the basis of a modification of the ECT method (MECT)[16]. Pins with an a spherical end supporting and loading the specimens were situated in opposite corners (Figure 4.b). The specimens were subjected to end torsion induced by a pair of counteracting moments at distance W . Each moment was generated by a pair of forces $P_{III}/2$ with a moment arm S . During the tests, the deflection of specimens δ_{III} was applied at a speed of 1 mm/min, and the parameter measured was force P_{III} .

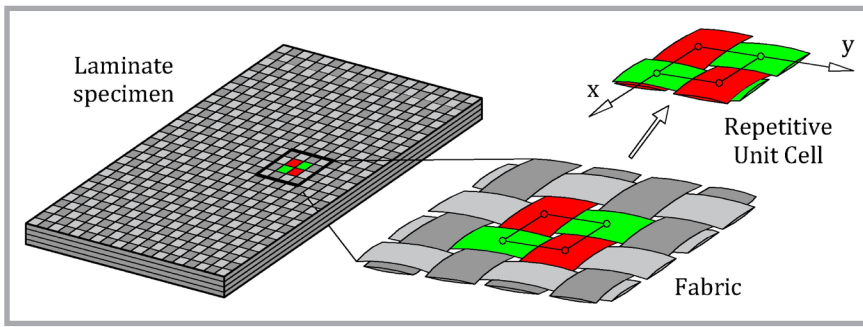


Figure 8. Repetitive Unit Cell (RUC) of the laminate modelled marked on the specimen and the fabric.

Table 1. Summary table of experimental results.

Delamination test	Point	Quantity, unit	Average value	Measurement uncertainty
DCB – (Figure 5.b)	MAX _I	Force $P_{I(MAX)}$, N	46.87	2.03
		Displacement $\delta_{I(MAX)}$, mm	4.23	0.26
ENF – (Figure 6.b)	NL _{II}	Force $P_{II(NL)}$, N	528.3	11.8
		Displacement $\delta_{II(NL)}$, mm	2.88	0.07
MECT – (Figure 7.b)	NL _{III}	Force $P_{III(NL)}$, N	784.31	33.61
		Displacement $\delta_{III(NL)}$, mm	6.64	0.37

Experimental results

In each case testing of specimen delamination according to the three basic fracture modes (Figure 1) was carried out for fifteen composite specimens. Results in the form of exemplary load-displacement curves of the specimens are shown in Figure 5.a, 6.a, and 7.a while the main purpose of the tests was to determine the averaged curves (Figure 5.b, 6.b, and 7.b).

In the case of the DCB test, one can distinguish two phases. In the first, the curves are linear (Figure 5.a). The initial delamination does not increase, and the specimens bend and accumulate the potential energy of deformation. In the second phase, a crack starts to propagate perpendicularly from the initial front of delamination, while the δ_I opening changes in a stepped manner in the function of force P_I . The size of the step corresponds to the span of the rovings in the reinforcement fabric. Between the stepped growths of the opening, relationship $P_I(\delta_I)$ is linear. On the basis of fifteen curves, an

averaged curve was determined for all the specimens for the linear range (Figure 5.b). After exceeding the critical force $P_{I(MAX)}$, which corresponds to the MAX_I point on the experimental curve, delamination starts and force P_I decreases to the FF_I point (first failure point).

On the averaged curve $P_{II}(\delta_{II})$ for the ENF test, three points are distinguished (Figure 6.b). Point NL_{II} (non-linear point) is the moment in which the curve changes from linear to non-linear. Furthermore the curve gently deviates from the linear one until the moment when the load reaches the critical value, which corresponds to the MAX_{II} point. After exceeding the critical force $P_{II(MAX)}$, intense crack growth is observed. Point VIS_{II} (visual observation point) corresponds to the moment in which one can visually observe progressive delamination on the lateral surface of the specimen.

On the averaged curve $P_{III}(\delta_{III})$ for the MECT test, three points are marked (Fig-

ure 7.b). At point NL_{III}, the linear plot changes to non-linear. It is worth adding that after exceeding this point, acoustic effects appear with increasing intensity, indicating progressive delamination. Furthermore a slight change in the curve is observed, which means a stable growth of delamination. Point 5%_{III} is at the intersection of the plot with the linear part of this plot, which is extended and deviated by 5%. After exceeding the critical force $P_{III(MAX)}$, which corresponds to point MAX_{III}, intense crack growth is observed.

Table 1 presents the average values of displacement and force for selected characteristic points. In each case, the average value was determined on the basis of the results of fifteen tests. Additionally, the table presents measurement uncertainty for each value at the level of confidence of $\alpha = 0.95$.

Finite element model

Engineering practice of computing strength and stiffness of constructions made of heterogeneous technical materials such as laminates reinforced with fabric layers expects from a computational model a compromise between the accuracy of modelling structure and the numerical efficiency of model analysis. When developing a discrete laminate model which allows simulation of its cracking under loading, thus determining its load capacity, it was assumed that the model should be useful in engineering calculations of real structures made of laminate. The consequence of this assumption was the adoption of the mesoscale laminate model, which is a satisfactory compromise between the level of detail reflecting the internal structure of the laminate and the numerical efficiency of the model. Since in the engineering calculations of real laminate structures it is difficult to predict the location of the crack initiation site in advance, the previously described delamination modelling techniques using the finite element method, such as VCCT

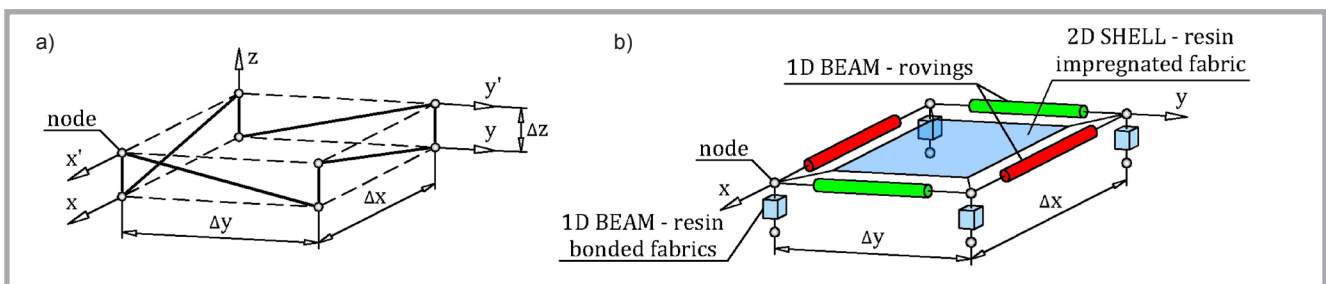


Figure 9. Repetitive Unit Cell (RUC) of the modelled laminate: a) in the form of a simplified scheme, b) in the form of a mesoscale model.

[9, 10], debonding [11, 12] or the cohesive zone [13, 14], were rejected.

It started with the isolation of the smallest repetitive part of the structure from the laminate, the so-called repetitive unit cell (RUC), which for a plain weave fabric consists of two pairs of interwoven rovings connected by the matrix (*Figure 8*). The way of crossing of the reinforcement rovings in a cell is shown in *Figure 9.a*, and its computational model requires defining eight nodes, four in the xy plane and four in the $x'y'$ plane. In order to simplify the cell model, the vertical shift of the roving interlace points was omitted, assuming that parameter Δz is small compared to dimensions Δx and Δy . Then the cell is defined by only four nodes lying in one plane (*Figure 9.b*). The segments of the reinforcement rovings between the nodes were modelled with beam type finite elements and the matrix between the nodes – with the shell type finite element. The connection of the cells of adjacent layers is also modelled with beam type finite elements.

Laminate is a construction material whose properties depend on manufacturing technology much more than those of metals. The way of forming parts from laminate affects the impregnation of the reinforcement with the matrix and the occurrence of structural defects such as bubbles and inclusions, resulting in differing characteristics of laminates made of the same components with the same reinforcement structure but in different conditions. The computational model of the laminate proposed makes it possible to take into account this variability by proper selection of cross-section parameters of the finite elements forming a repetitive unit cell (*Table 2*). This problem was solved by performing a calibration of the model consisting in the formulation of a parametric optimisation problem in which one sought the cross-sectional parameters of the beam elements and thickness of the shell element in closest compliance with the calculated and experimentally measured deflections of the laminate specimen made using a specific manufacturer's technology [5].

The possibility of easy modification of repetitive unit cells makes them useful in modelling composites with other reinforcement structures and orientations. The beam-shell model can be used to simulate the stiffness of composites with any orientation of the plain weave fabric

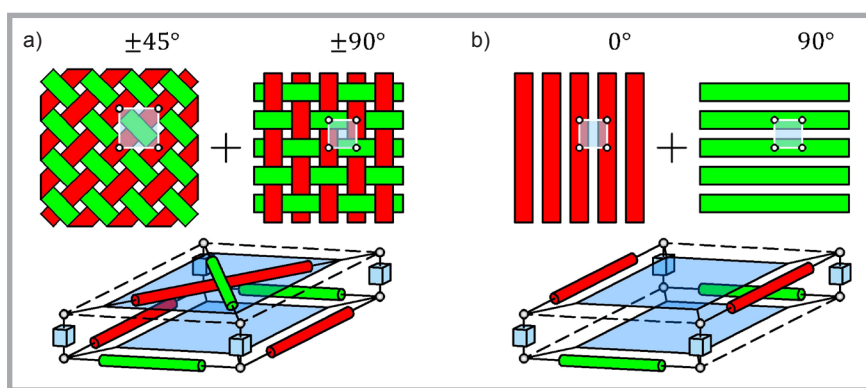


Figure 10. Mesoscale RUC model: a) for laminate reinforced with woven fabric of any layers configuration, b) for laminate with unidirectional layers of any configuration.

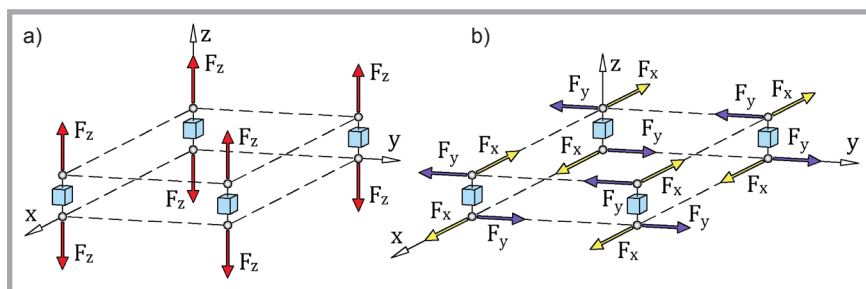


Figure 11. Simplified scheme of RUC: a) beam elements loaded with tensile forces; b) beam elements loaded with shear forces in two directions.

in each layer, but it is required to scale the fabric due to the different dimensions of the repetitive unit cells (*Figure 10.a*). Moreover, one can model a unidirectional laminate in the form of rovings or yarns arranged in a parallel manner in any configuration (*Figure 10.b*). The method of modelling laminates proposed can also be applied to laminates reinforced with fabric of other than plain weave, even ones reinforced with knit fabric if the repetitive unit cell is properly modified. The usefulness of the models developed in the analyses of the stiffness of laminate specimens was confirmed by experimental and computational tests [6].

Thanks to the structure of the repetitive unit cell, the computational models created with its help make it possible to simulate delamination. Initiation and development of the crack in the model can be the result of removing beam elements modelling the bondings between the fabric layers (cohesive separation of the reinforcement layers).

This procedure requires defining appropriate criteria which make it possible to select overloaded finite elements and then reduce their cross-section and/or remove them. In the case of the opening mode, the elements that are removed are those in which the criterion of the permissible tensile force F_z is exceeded (*Figure 11.a*). The condition of selection of beam elements during sliding and scissoring shear can be put on shear forces F_x and F_y , which contribute to the shear of the beam elements (*Figure 11.b*).

Numerical analyses

Mesoscale models of laminate specimens were generated by means of a special program using the Ansys APDL command language [11]. The program places nodes numbered according to the orthocartesian coordinate system adopted for the specimens, which are then connected by the finite elements according to the definition of the repetitive unit cell. The program

Table 2. Engineering constants and exemplary values of parameters for finite elements creating the RUC mesoscale model.

Finite element type	Young's modulus, MPa	Poisson's ratio, -	Area, mm ²	Area moment of inertia, mm ⁴	Thickness, mm
1D Beam – roving	105 000	0.1	0.12	0.065	–
1D Beam – resin	3400	0.35	1.56	0.2	–
2D Shell – resin	3400	0.35	4	–	0.04

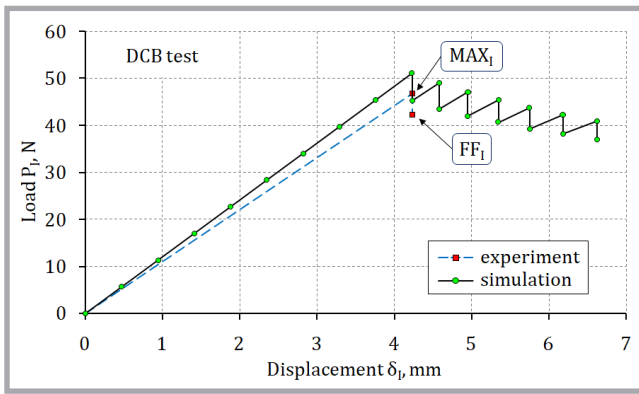


Figure 12. Comparison of the computational and experimental load-displacement curves for the DCB test.

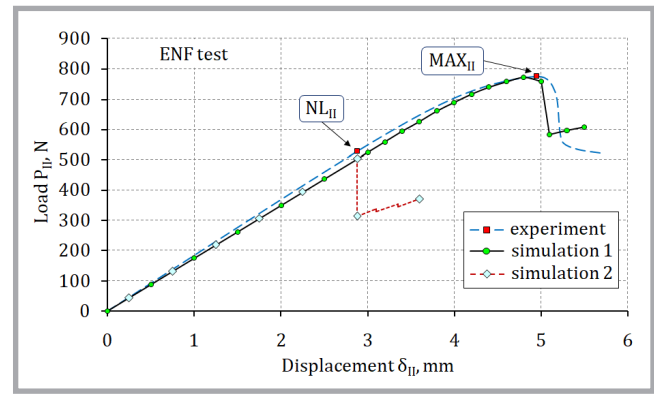


Figure 13. Comparison of the computational and experimental load-displacement curves for the ENF test.

assigns material constants of components and cross-section parameters to the elements, maintaining the volume shares of the components. The specimen models consisted of sixteen layers of nodes, which corresponded to the number of reinforcement layers. The pre-crack involved removing the beam elements modelling the resin between the middle layers of the model. The calculations were carried out with observance of the boundary conditions operative in the experimental studies. In each case, the program increased the displacement of nodes stepwise and recorded the value of nodal reactions. Between successive displacement growths, the algorithm checked the conditions of selecting beam type elements.

Delamination simulation in the conditions of the DCB test involved removing the selected element binding the layers in one step after exceeding the criterion of the threshold value of the tensile force F_z^k . The value of force F_z^k was determined on the basis of a trial simulation of the specimen model, which consisted in the reconstruction of the experiment. Its critical value corresponded to the tensile force in the first row of beam elements binding the middle layers at the moment of the MAX on the averaged experimen-

tal curve (Figure 5.b). The same was done in the case of ENF test simulation, with the difference that the structural force F_x^k was read for the deflection corresponding to the NL_{II} point (Figure 6.b).

Trial simulations of the ENF test showed that removing the elements in one step did not reflect the experimental curve closely enough. The effect of removing the first row of elements was that the criterion of the threshold value of the shear force was also met for the elements in the second row with an unchanged external load value, which resulted in intense crack growth. In order to obtain a better congruence between the results of calculations and the experiment, a procedure was suggested consisting in a stepwise reduction of the cross-sectional area of the beam elements binding the layers in several steps. After conducting a number of numerical tests, a rule was finally established according to which the reduction in cross-section A will take place in seven steps, in each of which the section will be reduced by 45% in relation to that in the previous step (the beam element is removed in the eighth step). This is tantamount to making an assumption that cross-section A_i in the succeeding steps of reduction (i is the number of reduc-

tion step) in relation to the initial section ($i = 0$) will be determined by a term of geometrical progression or by an exponential function (normalized values).

$$A_i = 0.55^i \vee A_i = e^{-0.60i} \text{ for } i = 1, 2, \dots, 7 \quad (1)$$

Such a procedure also required determining the threshold values of the shear force F_x^k (normalised values) in the succeeding steps of section reduction, which were also described by the geometrical progression and exponential function.

$$F_{xi}^k = 0.78^i \vee F_{xi}^k = e^{-0.25i} \text{ for } i = 1, 2, \dots, 7 \quad (2)$$

Due to the similarity of the delamination processes, in the simulation of the MECT test the same rule of reduction in the section of the elements bonding the layers was applied as in the ENF test simulation.

Results and discussion

On the basis of the simulations of laminate specimen delamination performed, curves were obtained in the force-displacement system, which were compared with the results of experimental tests. In the case of the DCB test, the crack propagation proceeded in a stepped manner, similar to the specimens during the experiment, with the intervals between succeeding steps being equal (Figure 12). The mode of delamination obtained resulted from the regular construction of the model, because the latter did not take into account the mutual displacement of the repetitive unit cells of the adjacent fabric layers. In general, a very good convergence was obtained between computational and experimental results. The coefficient of determination R^2 for the linear range in the case of the DCB test had the value of 0.86.

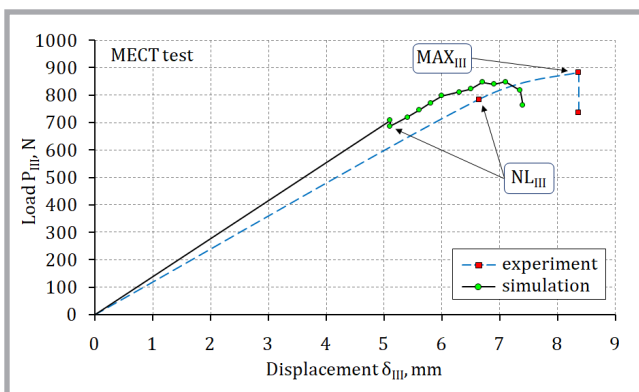


Figure 14. Comparison of the computational and experimental load-displacement curves for the MECT test.

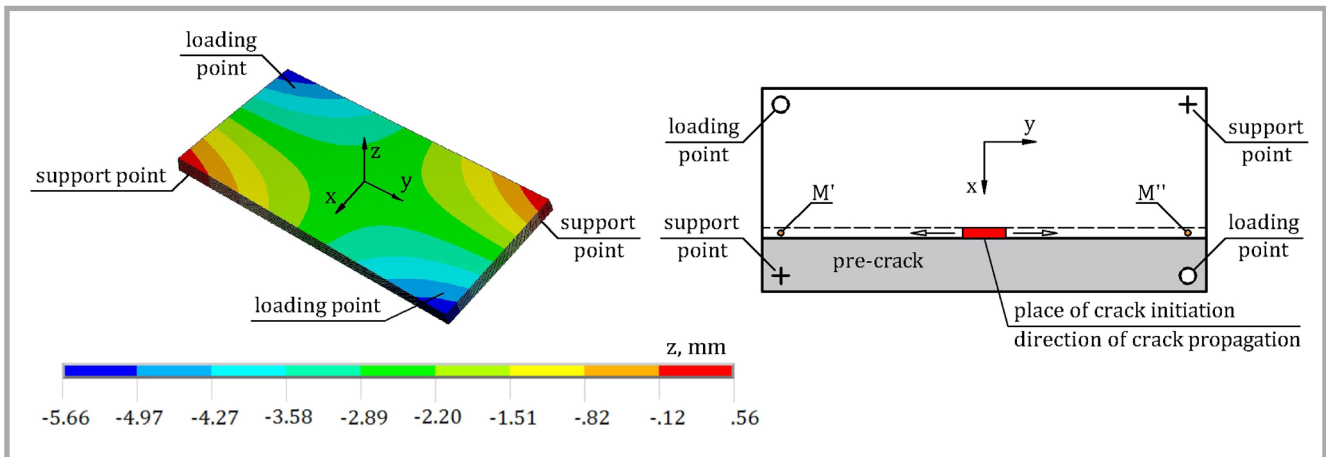


Figure 15. Simulation results for the MECT test and direction of the crack growth in the FE model.

A similar convergence of results was obtained for the ENF test carried out with the use of ASTM D790 standard. The coefficient of determination R^2_{II} in the range measured from 0 to point MAX_{II} had the value of 0.97 – simulation 1 (Figure 13). The plot also presents the computational curve of the model, in which the algorithm removed the beam elements in one step, omitting the stepwise section reduction – simulation 2. At the moment of initiation of delamination, which corresponded to point NL_{II} on the averaged experimental curve, the model showed a jumped crack growth. Such a course of the numerical experiment was discordant with the experiment.

In the case of the MECT test, the crack growth in the model began before the experimental point NL_{III} (Figure 14). The computational curve slightly deviated from the experimental one. The first crack in the model appeared in the middle of the specimen length (Figure 15). The propagation of the crack proceeded along the edges of the initial delamination from the centre towards the outer edges of the specimen. In the beam elements binding the layers near points M' and M'' , additional shear forces occurred for the II fracture mode, but their value was smaller than the threshold value.

Conclusions

- The shell-beam laminate FE model for technical materials such as laminates reinforced with fabrics takes into account the micro-structure at the component level – rovings and matrix as well as the internal laminate structure.
- The model does not require predicting the places of delamination occurrence

because the initiation and growth of a crack may occur in any place.

- The model can reflect the stiffness and strength of the laminate with an accuracy acceptable in engineering calculations, and it is also effective enough numerically.
- The model takes into account the production conditions and makes it possible to reconstruct laminate behaviour under a load based on the knowledge of properties of components, their volumetric share as well as on knowledge of substitutionary cross-section parameters of the finite elements.
- The model's adequacy to reality was confirmed by the experiments conducted, the results of which were in accordance with the calculation results.

References

1. Azzam A, Li W. Experimental investigation on the impact behaviour of composite laminate. *FIBRES & TEXTILES in Eastern Europe* 2015; 23, 1(109): 77-84.
2. Bednarczyk BA, Stier B, Simon J-W, Reese S, Pineda EJ. Meso- and micro-scale modeling of damage in plain weave composites. *Composite Structures* 2015; 121: 258-270.
3. Goda I, Assidi M, Ganghoffer J-F. Equivalent mechanical properties of textile monolayers from discrete asymptotic homogenization. *Journal of the Mechanics and Physics of Solids* 2013; 61: 2537-2565.
4. Gatouillat S, Bareggi A, Vidal-Sallé E, Boisse P. Meso modelling for composite preform shaping – Simulation of the loss of cohesion of the woven fibre network. *Composites: Part A* 2013; 54: 135-144.
5. Stadnicki J, Tokarz Z. Mesoscale finite element model for calculating deformations of laminate composite constructions. *Advances in Mechanical Engineering* 2016; 8(2): 1-9.
6. Marszałek J. Mezoskalowe modele MES kompozytów o zmiennej orientacji warstw wzmocnienia. *Przegląd Mechaniczny* 2017; 7-8: 39-41.
7. Soni G, Singh R, Mitra M, Falzon BG. Modelling matrix damage and fibre-matrix interfacial decohesion in composite laminates via a multi-fibre multi-layer representative volume element (M^2RVE). *International Journal of Solids and Structures* 2014; 51: 449-461.
8. Jia X, Xia Z, Gu B. Nonlinear viscoelastic multi-scale repetitive unit cell model of 3D woven composites with damage evolution. *International Journal of Solids and Structures* 2013; 50: 3539-3554.
9. de Moraes AB, Pereira AB. Mixed mode II + III interlaminar fracture of carbon/epoxy laminates. *Composites Science and Technology* 2008; 68: 2022-2027.
10. Liu PF, Islam MM. A nonlinear cohesive model for mixed-mode delamination of composite laminates. *Composite Structures* 2013; 106: 47-56.
11. ANSYS Inc., ANSYS Mechanical APDL Theory Reference ver. 17.2; 2016.
12. Skvortsov YuV, Chernyakin SA, Glushkov SV, Perov SN. Simulation of fatigue delamination growth in composite laminates under mode I loading. *Applied Mathematical Modelling* 2016; 40:7216-7224.
13. Lindgaard E, Bak BLV, Glud JA, Sjølund J, Christensen ET. A user programmed cohesive zone finite element for ANSYS Mechanical. *Engineering Fracture Mechanics* 2017; 180: 229-239.
14. Naghipour P, Schneider J, Bartsch M, Hausmann J, Voggenreiter H. Fracture simulation of CFRP laminates in mixed mode bending. *Engineering Fracture Mechanics* 2009; 76: 2821-2833.
15. Carlsson LA, Adams DF, Pipes RB. *Experimental characterization of advanced composite materials – fourth edition*. CRC Press, Boca Raton, FL, 2014.
16. Marat-Mendes R, de Freitas M. Characterisation of the edge crack torsion (ECT) test for the measurement of the mode III interlaminar fracture toughness. *Engineering Fracture Mechanics* 2009; 76: 2799-2809.

Received 04.04.2018 Reviewed 25.04.2018